Preprints, 4th IFAC Conference on
Advances in Proportional-Integral-Derivative Control
Almería, Spain | June 12-14, 2024

Classic PID-based control strategies for raceway photobioreactor biomass concentration and water level ⋆

Pablo Otálora * **Ángeles Hoyo** * **Malena Caparroz** *
José González * **José L. Guzmán** * **Manuel Berenguel** *

* *Department of Informatics, University of Almería, CIESOL, ceiA3, 04120 Almería, Spain (e-mail: {p.otalora, angeles.hoyo, mcaparroz, j.gonzalez, joseluis.guzman, beren}@ual.es).*

Abstract: This paper presents the simulation implementation of classical control strategies based on PID controllers for the simultaneous control of water level and biomass concentration in open reactors by manipulating the dilution (inflow) and harvested (outflow) flow rates. The system studied is a TITO (two inputs-two outputs) process with coupling between its variables, and a significant amount of disturbances, such as solar radiation, relative humidity and ambient temperature. The proposed strategies combine Controlled Variable (CV) and Manipulated Variable (MV) switching strategies to follow both setpoints and overcome saturation problems. A simulation of six consecutive days with different external climate conditions was performed. The results show that the proposed schemes can significantly improve the basic PID control performance. The proposed solutions are simple and generic, and behaving properly for both controlled variables.

Keywords: PID control, microalgae photobioreactors, control PID structures, selective control.

1. INTRODUCTION

The industrial production of microalgae has acquired significant relevance in a multitude of fields, from the food to the energy industry, including wastewater treatment and carbon dioxide fixation (Razzak et al. (2023)). The composition of their biomass, along with their high growth rate, makes them a very interesting and sustainable product. Microalgae production can be performed in open or closed reactors. Closed reactors allow for tighter control of culture conditions and prevent the entry of external contaminants, although they are more expensive and less scalable. Open reactors, on the other hand, are the most widely adopted due to their lower costs, albeit they have the disadvantage of being more susceptible to changes in climatic conditions (Egbo et al. (2018)).

Both the economic and energetic efficiency of the process go hand in hand with its productivity. The microalgae growth rate is closely dependent on culture conditions, particularly on the solar radiation, water temperature, pH, dissolved oxygen, and nutrient concentration. Therefore, it is critical to control these variables in order to optimize the process (Guzmán et al. (2021)).

Nevertheless, since it is a biological process constantly exposed to the environment, its highly changeable nature makes its modeling and optimization considerably difficult. For this reason, models based on first principles are often too complex and require periodic recalibration. Simpler models are unable to account for all the factors that influence the process, making it difficult to implement predictive control algorithms.

Under these circumstances, PID control is presented as a simple and robust alternative. However, the multiple interactions between the different variables demand the implementation of strategies that guarantee a desirable behavior in the system. This article compares multiple alternative control schemes based on PID controllers for the simultaneous control of water level and biomass concentration in open reactors by manipulating the dilution (inflow) and harvested (outflow) flow rates (Skogestad (2023)). The two controlled variables are highly coupled and have a significant impact on system productivity. The results demonstrate how simultaneous control of both variables with PID-based strategies is not only possible, but also more practical and reliable than other alternatives based on model predictive control.

2. MATERIALS AND METHODS

2.1 Raceway reactor

The modeled reactor used for this work is located in the facilities of the IFAPA research center at the University of Almería, Spain (see Fig. 1). The raceway reactor consists of two 40 m long and 1 m wide channels connected at their ends by 180º bends, through which the medium with the microalgae flows. The reactor has a paddle wheel that drives the fluid, as well as a sump through which CO_2 and air are injected to control the culture conditions. There are sensors to measure culture conditions, as well as biomass concentration, water level, and climatic variables,

⋆ This work has been financed by the PID2020–112709RB-C21 project financed by the Spanish Ministry of Science.

including radiation, ambient temperature, wind speed, and relative humidity. Data from these sensors are recorded 24 hours a day with a sampling time of one second.

Fig. 1. Raceway reactor located at IFAPA

2.2 Biological model

The dynamic model in a raceway photobioreactor is composed of a biological model describing the growth rate of the microalgae and an engineering model describing mass transfer, heat transfer, and biological phenomena occurring in the different parts of the reactor. All these models have been developed and validated in (Bernard and Rémond, 2012; Ippoliti et al., 2016; Fernández et al., 2016; Sánchez-Zurano et al., 2020), and used here as the plant simulator.

Regarding the biological model, microalgae production is based on the photosynthesis rate balance P_{O_2}. It is calculated with a function of four terms as shown in equation (1). These are the average light term $P_{O_2}(I_{av})$, the medium temperature $\overline{P_{O_2}(T)}$, the medium pH $\overline{P_{O_2}(pH)}$ and the dissolved oxygen concentration $\overline{P_{O_2}(DO)}$. The average light term is a quantitative factor representing the oxygen production per biomass unit and time. In contrast, the rest of the terms are dimensionless and normalized with values between 0 and 1.

$$P_{O_2} = P_{O_2}(I_{av}) \cdot \overline{P_{O_2}(T)} \cdot \overline{P_{O_2}(pH)} \cdot \overline{P_{O_2}(DO)} \tag{1}$$

The terms related to temperature, $\overline{P_{O_2}(T)}$, and pH, $\overline{P_{O_2}(pH)}$, reach their maximum value when the variable on which they depend is at an optimum value specific to the produced strain, reducing the photosynthesis rate proportionally to the difference from this optimum value. On the other hand, the term related to dissolved oxygen, $\overline{P_{O_2}(DO)}$, decreases as this variable increases, although in a milder way for low values, becoming more accentuated the more its value increases.

Average light-based productivity, $P_{O_2}(I_{av})$, is defined in equation (2). It is calculated as a function of several parameters specific to the microalgae strain and the growth state of the cells. $P_{O_2,max}$ is the maximum photosynthetic rate defined by the culture conditions, n is a shape exponent, I_k is the minimum amount of light needed by the microalgae to achieve maximum photosynthesis, and I_{av} is the average solar radiation available to the microalgae. This average solar radiation integrates the value of the local radiation along the reactor. It is calculated as shown in equation (3). As can be seen, the radiation received by the microalgae I_{av} depends on the incident radiation on the reactor surface I_0, as well as on the water level h and the biomass concentration C_b. K_a is a parameter related to the biomass light attenuation. If these variables adopt excessively high values, the culture will receive significantly less light, and, consequently, its growth will be reduced.

$$P_{O_2}(I_{av}) = \frac{P_{O_2,max} I_{av}^n}{I_k^n + I_{av}^n} \tag{2}$$

$$I_{av}(t) = \frac{I_0(t)}{K_a C_b(t) h(t)} \left(1 - e^{-K_a C_b(t) h(t)}\right) \tag{3}$$

From this photosynthesis rate, it is possible to establish an equation that describes the evolution of the biomass concentration over time, taking into account the mechanisms that increase or decrease the biomass in the reactor without affecting the volume of water, and those that modify the volume of water without changing the total biomass. This can be seen in (4), where $Q_D(t)$ is the dilution flow rate, $g_s(t)$ is the evaporation rate, and $V(t)$ is the total volume of water in the reactor. Note that the biomass concentration will increase during the hours when photosynthesis takes place, and decrease during dilution. The effect of evaporation is often negligible.

$$\frac{dC_b(t)}{dt} = C_b(t) \left(P_{O_2}(t) - \frac{Q_D(t) - g_s(t)}{V(t)}\right) \tag{4}$$

The evolution of the water level in the reactor is simple to describe, taking into account the addition of medium by dilution and its removal by harvesting $Q_H(t)$ and evaporation, as shown in equation 5, where A is the area of the reactor.

$$\frac{dh(t)}{dt} = \frac{1}{A} \left(Q_D(t) - Q_H(t) - g_s(t)\right) \tag{5}$$

For the purpose of this work, these two equations, along with the photosynthetic rate equations, are sufficient to describe the system. The water level and the biomass concentration will be considered as controlled variables (CVs), while the harvesting and dilution flow rates will be considered as the manipulated variables (MVs). The actual values of medium temperature, pH and dissolved oxygen for the days studied will be used, during which control over the latter two variables was performed, as well as the actual values of the climatological variables. Therefore, the system studied is a TITO system (two inputs-two outputs) with a significant amount of disturbances, such as solar radiation, relative humidity and ambient temperature, and coupling between its variables.

3. CONTROLLER DESIGN

This section presents the different control schemes applied for the control problem presented in this work. Five classic control strategies have been implemented to control the water level (h) and the biomass concentration (C_b) of the raceway reactor, as described below.

In order to tune the controllers, three linear models describing the relationship between the inputs and outputs of the system around the desired operating point were identified, shown in equations (6), (7) and (8). The effect of

harvesting and dilution on the water level is the same with opposite sign on the gain $[cm/(L/min) \cdot s^{-1}]$, operating as an integrator, as can be inferred from equation (5). The effect of dilution on biomass concentration is described by a first-order transfer function with negative gain $[(g/L)/(L/min)]$ and a remarkably high time constant $[min]$, while harvesting does not have a direct effect on this variable.

$$P_{h,Q_H}(s) = \frac{H(s)}{Q_H(s)} = \frac{-2.083}{s} \tag{6}$$

$$P_{h,Q_D}(s) = \frac{H(s)}{Q_D(s)} = \frac{2.083}{s} \tag{7}$$

$$P_{C_b,Q_D}(s) = \frac{C_b(s)}{Q_D(s)} = \frac{-0.0079}{181.33s + 1} \tag{8}$$

All the controllers in this section are defined as PI controllers (Visioli (2006); Åström and Hägglund (2006)). Supplementary elements such as anti-windup and constraints (input limits) have been implemented. They have been tuned with the SIMC tuning rule (Skogestad, 2003). All strategies have been set with the same closed-loop time constant to be compared. Therefore, the controller parameters for the controllers C_h or C_{h_1} and C_{C_b} are: $K_{p,h} = -66.67\,[(L/min)/cm]$, $T_{i,h} = 48\,[min]$, $K_{p,C_b} = -1534\,[(L/min)/(g/L)]$ and $T_{i,C_b} = 60\,[min]$. The controller parameters of C_{h_2} are: $K_{p,h_2} = 66.67\,[(L/min)/cm]$, $T_{i,h_2} = 48\,[min]$, and the controller parameters of C_{Q_h} are: $K_{p,Q_h} = 1\,[-]$, $T_{i,Q_h} = 36\,[min]$. Some modifications that happen in some of them are explained in detail below.

The main objective of the controller is to keep its CV close to a given setpoint by affecting its MV. Given that the studied system is a TITO system, it is mandatory to couple the CVs and the MVs. This has been done by following the 'pair-close rule', in a way that each MV is paired with the CV that it affects the most. This way, the dilution flow rate has been paired with the biomass concentration, as it is the only MV that affects this CV; and the harvesting flow rate has been paired with the water level. This pairing, although theoretically valid, has some limitations in practice related to the saturation of the MVs and the difficulty in reaching the setpoints under certain circumstances. This difficulty can be addressed through some of the schemes presented below.

3.1 PID Schemes

In this subsection, the five different control schemes that have been implemented are explained in detail. The closed-loop time constants of the PI controllers have been set to $\tau_{cl,h} = 12\,[min]$ and $\tau_{cl,c_b} = 15\,[min]$, for the level control and biomass concentration control, respectively, for all the control schemes. These values have been chosen based on previous experience with the process.

Classic PID scheme

This scheme is based on two classic feedback PI controllers, as shown in Fig 2. In this setup, two different PI controllers, C_{C_b} and C_h, for the biomass concentration control and level control, respectively. While the simplicity of this approach stands as its main advantage, its performance may be compromised due to the interaction between variables inherent in the MIMO processes.

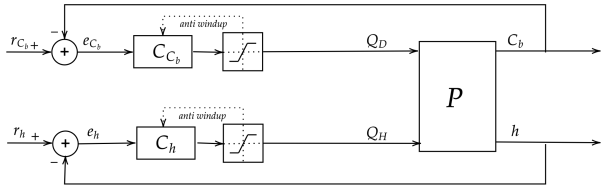

Fig. 2. Block diagram with classic separated PI controllers.

Linear decoupling in classic PID scheme

As defined in the previous section, due to the TITO nature of the system, the process outputs are coupled. On the one hand, a change in the dilution flow affects the concentration and water level. However, the harvest flow only modifies the water level. In this case, to avoid the interaction between dilution and harvesting, a linear decoupling is implemented and calculated as defined in equation (9). Fig. 3 shows the proposed linear decoupling with the classic PID scheme.

$$D(s) = -\frac{P_{h,Q_D}(s)}{P_{h,Q_H}(s)} = 1 \tag{9}$$

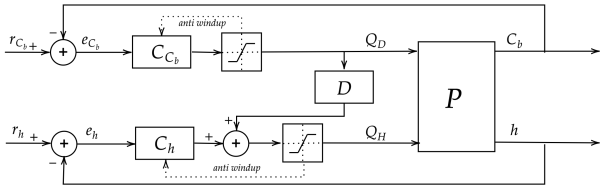

Fig. 3. Block diagram for linear decoupling in classic PID control scheme.

Split range control for MV-MV and CV switching with max selector

This scheme implements a split range control for the manipulated variables, as shown in Fig. 4. A maximum selector switch has also been incorporated to select between two control variables.

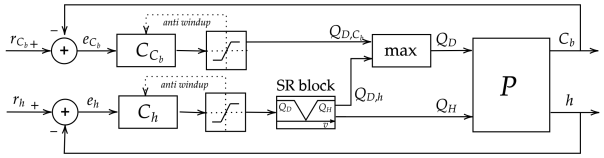

Fig. 4. Block diagram with split range control for MV ($Q_{D,h}$) - MV (Q_H) for level control problem and a max selector on MV (Q_D).

In this case, the system is first analyzed as a MISO (multi-input single-output) system for the water level output, which has two manipulated variables (Q_H and Q_D) for one output variable (h). The aim is to control the system's water level using both the harvested and dilution flows. To prevent simultaneous adjustments, the split range control is designed where a single controller will compute the internal signal v. This signal enters the split range block, determining the harvesting or dilution flow (manipulated variables), based on the scheme shown in Fig. 5.

Furthermore, a maximum selector has been implemented to select the manipulated variable Q_D, which will have two different values, one from the water level control ($Q_{D,h}$), and the other from the biomass concentration control (Q_{D,C_b}). Fixing it to the maximum value ensures that the concentration does not exceed the set value. Still, it may fall below if necessary for level control.

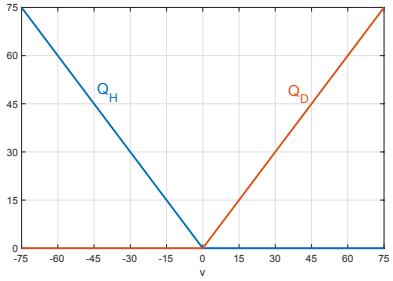

Fig. 5. Internal signal to split range (SR) block.

Separate controllers for MV-MV switching and CV switching with max selector

This solution implements an alternative to the split range control described above, where two separate controllers are designed for each MV ($Q_{D,h}$, Q_H) that affects the water level (Smith (2011); Reyes-Lúa and Skogestad (2019)). The implemented scheme is shown in Fig. 6. This scheme allows to maintain the water level around the desired setpoint with a tolerance of $\Delta r_h = 0.2$. This control is not as tight in terms of following the setpoint, but it allows independent tuning of the controllers of each of the MVs, in case their dynamics with respect to the CV are different. The closed-loop time constants for each controller were set as in the previous schemes, that is, $\tau_{cl,h_1} = 12\,[min]$, $\tau_{cl,h_2} = 12\,[min]$ and $\tau_{cl,c_b} = 15\,[min]$.

As in the split range control scheme, a maximum selector has also been implemented to select the manipulated variable Q_D from the level or concentration controller.

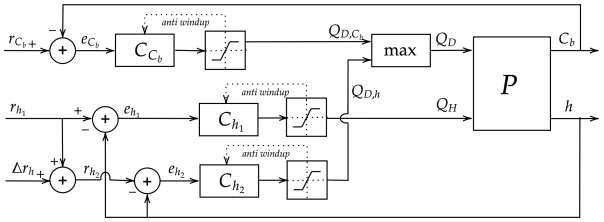

Fig. 6. Block diagram for separate controllers for MV ($Q_{D,h}$) - MV (Q_H) switching and a max switch with selector on MV (Q_D).

Valve Position Control (VPC) for MV-MV switching and CV switching with max selector

In this scheme, a new controller (C_{Q_H}) is implemented to control the harvesting flow rate Q_H, as shown in Fig. 7. In this case, the water level loop presents two controllers: the first one (C_{C_b}) acting on Q_H to follow the level setpoint, and the second one (C_{Q_H}) acting on the Q_D, in charge of bringing Q_H to a small value, slightly higher than 0. This scheme ensures proper level control using both MVs, with the small drawback that Q_H will be used even in steady state. However, this feature may be of interest in cases where a minimum dilution rate must be guaranteed regardless of disturbance rejection. To design the new controller, a new model that relates the harvesting and dilution flow is needed. Equation (10) represents its transfer function, where an approximation with the half-time rule (Skogestad (2003)) is made.

$$P_{Q_H,Q_{D_h}} = -\frac{C_{C_b} P_{h,Q_D}}{1 + C_{C_b} P_{h,Q_H}} = \frac{48s+1}{(120s+1)(120s+1)}$$
$$P_{Q_H,Q_{D_h}} \approx \frac{48s+1}{(180s+1)} e^{-60s} \tag{10}$$

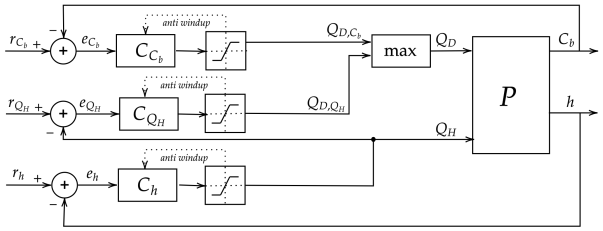

Fig. 7. Block diagram for VPC MV ($Q_{D,h}$) - MV (Q_H) switching and a max switch with selector on MV (Q_D).

4. RESULTS

This section presents the simulation results for the five previous control algorithms, where the nonlinear model described in Section 2 was used as simulator.

The Integral Absolute Error (IAE) metric was used to evaluate and compare the performance of the different control approaches. The IAE for each control scheme has been normalized with respect to the classic PID scheme.

A simulation of six consecutive days with different weather conditions was performed. The used weather and culture conditions data were obtained from the real reactor defined in Section 2 in April 2023. The tests have been set as follows: two days in the steady state around the optimal operating point, two days with a step change in the concentration setpoint r_{C_b} from 0.65 g/L to 0.74 g/L, and two days with a step change in the level setpoint r_h from 15 cm to 14 cm. These steps were performed during the central hours of the day to ensure minimum dilution of the reactor, as well as to prioritize harvesting during the last hours of the day. The simulation results are shown in Fig. 8, and the IAE indices in Table 1.

Table 1. Normalized IAE indices for water level (IAE_h) and biomass concentration (IAE_{C_b}).

	IAE_h	IAE_{C_b}
Decoupling PID	0.41	0.99
Split Range	0.18	1.69
Separate controllers	1.11	1.01
VPC	0.93	1.09

Starting with the days without step changes, Fig. 8 shows that the setpoint values are stationary on the first and fourth days. However, the concentration begins the first day below the optimal reference value, and the control is activated to bring it to the desired value, keeping both

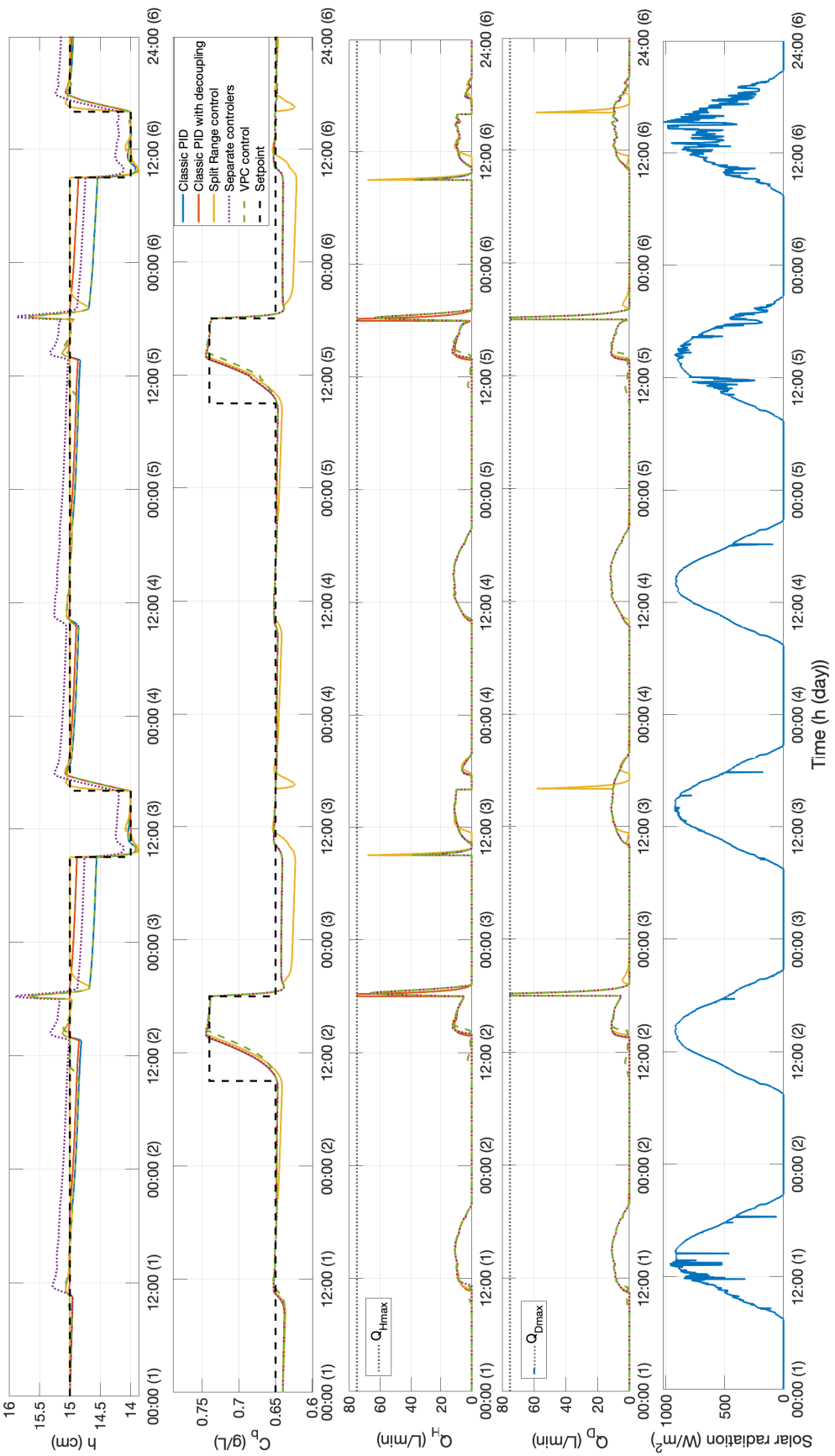

Fig. 8. Simulation results for six consecutive days with step reference changes on water level and biomass concentration.

variables at the setpoint. All the control strategies behave similarly except for the separate controllers, the one with more error on the water level. The MV profiles are smooth, following the shape of the solar radiation curve.

On the days with a setpoint step change in biomass concentration, which are the second and fifth days, it can be observed how each scheme correctly follows up on the reference at the first step. However, when returning to the optimal value at the end of the day, the biomass concentration value is below the reference value in most control strategies. This is because of the lack of radiation, which causes the concentration to not rise enough to reach the reference; it being the split range control the one with the most error as it is the one that keeps the water at the setpoint. As a result of the dilution flow rate necessary to achieve this, the concentration value is lowered more than with the rest of the controllers. Regarding the level control, which is now a disturbance rejection problem due to the concentration step change, the controller that obtains the lowest error is the PID controller with decoupling, completely rejecting the disturbance in trade for a more aggressive control signal, as the decoupling transfer function is dinamically accurate. The VPC control presents the highest error during this time.

The third and sixth days, presenting a step change in the level setpoint, show that similar reference tracking is performed for every strategy except for the split range control scheme. The biomass concentration behaves similarly in all strategies, staying almost at the reference value throughout the test despite the disturbances caused by the level change. The control signals for harvesting and dilution flow rates are alike for all the schemes, with the exception of the dilution flow rate from the split range control in which a high control signal occurs when returning to the optimal level value, reaching the setpoint faster as a consecquence. This can be noticed as a momentary drop on the biomass concentration, result of such sudden dilution.

Observing the normalized IAE indices in Table 1 for each output, the output performance of each control strategy can be analyzed. Decoupling is the most balanced control scheme regarding the IAE index compared to PID. However, it has the disadvantage of having the most aggressive control signal. Furthermore, the split range is the one with the slightest error in level control, thus penalizing the concentration control, especially at night, since during this period the concentration cannot rise while the water level drops due to evaporation. It improves the PID by 82% on the performance of the level control. The separate controllers scheme is the most flawed performer overall, as its level specification is more loose. The VPC control strategy behaves very similarly to the PID control, both in the level and concentration IAE index.

5. CONCLUSION

This work has presented the simulation implementation of different classical control strategies for biomass concentration and level control in a raceway reactor. Classical PID control, PID plus decoupling, split range control, separate controllers, and VPC control have been implemented and compared in simulation.

With the changes in both the level and concentration setpoints, it has been observed how each strategy independently prioritizes the control of one of the two output variables. Each strategy manages to keep the biomass concentration value below its setpoint, as specified. Still, similar results have been obtained from them. This study allows for the establishment of a simple, precise and generic strategy for the simultaneous control of both variables, serving as a basis for its implementation in real photobioreactors, intended to be carried out in future works. Similarly, the specific characteristics of each of the strategies can make them valuable for the control of other relevant process variables, such as pH or dissolved oxygen.

REFERENCES

Åström, K.J. and Hägglund, T. (2006). *Advanced PID control*. ISA - The Instrumentation, Systems and Automation Society.

Bernard, O. and Rémond, B. (2012). Validation of a simple model accounting for light and temperature effect on microalgal growth. *Bioresource Technology*, 123, 520–527.

Egbo, M., Okoani, A., and Okoh, I. (2018). Photobioreactors for microalgae cultivation–an overview. *Int J Sci Eng Res*, 9, 65–74.

Fernández, I., Acién, F.G., Guzmán, J.L., Berenguel, M., and Mendoza, J.L. (2016). Dynamic model of an industrial raceway reactor for microalgae production. *Algal Research*, 17, 67–78.

Guzmán, J.L., Acién, F., and Berenguel, M. (2021). Modelado y control de la producción de microalgas en fotobiorreactores industriales. *Revista Iberoamericana de Automática e Informática industrial*, 18(1), 1–18.

Ippoliti, D., Gómez, C., Morales-Amaral, M., Pistocchi, R., Fernández-Sevilla, J., and Acién, F.G. (2016). Modeling of photosynthesis and respiration rate for *Isochrysis galbana* (T-Iso) and its influence on the production of this strain. *Bioresource Technology*, 203, 71–79.

Razzak, S.A., Bahar, K., Islam, K.O., Haniffa, A.K., Faruque, M.O., Hossain, S.Z., and Hossain, M.M. (2023). Microalgae cultivation in photobioreactors: sustainable solutions for a greener future. *Green Chemical Engineering*.

Reyes-Lúa, A. and Skogestad, S. (2019). Multiple-input single-output control for extending the steady-state operating range—use of controllers with different setpoints. *Processes*, 7(12), 941.

Skogestad, S. (2003). Simple analytic rules for model reduction and pid controller tuning. *Journal of process control*, 13(4), 291–309.

Skogestad, S. (2023). Advanced control using decomposition and simple elements. *Annual Reviews in Control*, 56, 100903.

Smith, C.L. (2011). *Advanced process control: beyond single loop control*. John Wiley & Sons.

Sánchez-Zurano, A., Serrano, C., Acién, F.G., Fernández-Sevilla, J.M., and Molina-Grima, E. (2020). Modeling of photosynthesis and respiration rate for microalgae–bacteria consortia. *Biotechnology and Bioengineering*, 118(2), 952–962.

Visioli, A. (2006). *Practical PID control*. Springer Science & Business Media.